Carbon-coated copper nanoparticles: synthesis, characterization and optical properties†

Jing Li[a] and Chun-yan Liu*[b]

Received (in Victoria, Australia) 3rd April 2009, Accepted 28th May 2009
First published as an Advance Article on the web 5th June 2009
DOI: 10.1039/b906796e

Carbon-coated copper (C/Cu) nanoparticles with a size of 50–80 nm were synthesized through a simple solid-state reduction reaction. The reaction process and optical properties were subsequently explored.

Metallic nanoparticles are attracting increasing interest as an important class of photonic component to control and manipulate light at the nanometer scale.[1–4] When metal nanoparticles are excited by electromagnetic radiation, their conduction electrons' collective oscillations behave as surface plasmon resonance (SPR) and produce surface plasmons (SPs) spread across the surface of the particles. By altering the surface structure of the metal, the properties of the SPs, in particular their interaction with light, can be tailored. Plasmonic excitations provide a means to focus light to a subwavelength dimension, which would overcome the optical diffraction limit and enable the design of nanoscale optical devices, such as waveguides.[3,5] The intense local electromagnetic fields of metallic nanostructures accompanying plasmon resonance can also be exploited for surface enhanced spectroscopies.[6,7]

Theoretical studies and experimental work have suggested that SPR is influenced by many factors, including the size, concentration and shape of the metal particles, the dielectric function of surrounding materials, and so on.[8–10] Noble metal nanoparticles, such as Au and Ag, have been of particular interest for plasmonics because their plasmon resonance energy is in the ultraviolet and visible regions of the electromagnetic spectrum,[11] and they are much more stable compared with Cu and Al nanoparticles in the atmosphere. However, in comparison with noble metal nanoparticles (Pt, Au and Ag), Cu nanoparticles have their own distinguishing characteristics of lower cost and near-infrared plasmon resonance energy.[12] In previous work, Cu nanoparticles were synthesized in reverse micelles,[12–14] with organometallic precursors[15] and by photocatalytic methods.[16] These synthesized nanoparticles could be easily oxidized in air, forming an oxidation layer on the particle surface.

Carbon-coated nanomaterials, especially metals, are of great significance due to their stability to oxidation and degradation. There are various known methods to obtain a carbon coating on metal nanoparticles, the most popular being the arc-discharge technique.[17] Jacob and co-workers[18] synthesized carbon-coated core–shell-structured Cu nanoparticles by microwave irradiation in an ionic liquid, whereas the prepared nanoparticles aggregated together completely and could not be used in SPR studies.

In the present work, we synthesized carbon-coated Cu nanoparticles (C/Cu) by a simple solid-state reduction reaction of glucose ($C_6H_{12}O_6{\cdot}H_2O$) and cupric carbonate ($CuCO_3{\cdot}Cu(OH)_2{\cdot}xH_2O$), and studied the influence of a carbon coating on their SPR properties.

The fundamental reactions involved in our work can be simplified as follows:

$$CuCO_3 \cdot Cu(OH)_2 \cdot xH_2O \xrightarrow{350^\circ C} 2CuO + CO_2\uparrow + (x+1)H_2O\uparrow \quad (1)$$

$$C_6H_{12}O_6 \cdot H_2O \xrightarrow{350^\circ C} 6C + 7H_2O\uparrow \quad (2)$$

$$CuO + C \xrightarrow{350^\circ C} Cu + CO\uparrow \quad (3)$$

As is known, glucose starts to melt above 150 °C, and then undergoes a melting and carbonization process.[19] In our experiments, melting glucose acted as a dispersed medium where cupric carbonate particles were encapsulated. As the temperature increased, the cupric carbonate began to decompose and formed copper oxide, and the melting glucose carbonized and formed carbon, respectively. The carbon, as a reductant,[18] reduced the copper ions to pure Cu nanoparticles and synchronously formed a shell around them. The formation process is schematically described as follows (Fig. 1):

The thermal analysis curves (TG and DSC) of the sample are presented in Fig. 2. The DSC curve shows an endothermic profile from 245.5 to 348.7 °C, with a peak at 321.3 °C corresponding to the weight loss stage of TG, where cupric carbonate experienced a thermal decomposition process and

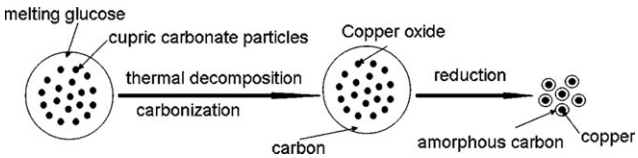

Fig. 1 Schematic illustration of the formation process of C/Cu.

[a] *Key Laboratory of Photochemical Conversion and Optoelectonic Materials of Technical Institute of Physics and Chemistry, Chinese Academy of Sciences, Zhongguancun, Beijing 100190, P. R. China*
[b] *Graduate School of the Chinese Academy of Sciences, Beijing 100806, P. R. China. E-mail: cyliu@mail.ipc.ac.cn*
† Electronic supplementary information (ESI) available: TEM images of the products synthesized with different amounts of glucose. See DOI: 10.1039/b906796e

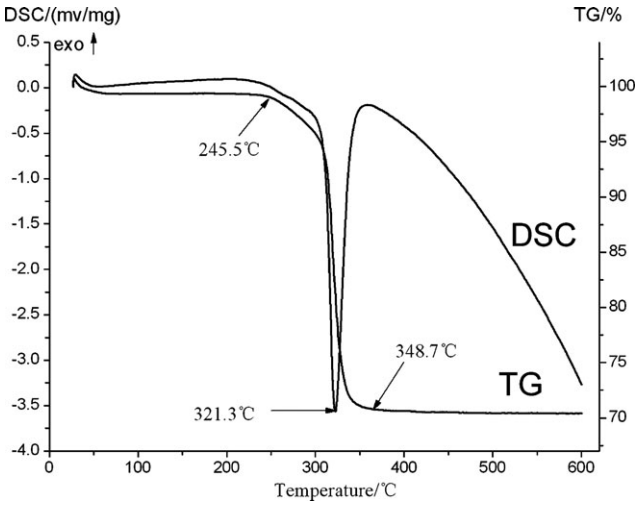

Fig. 2 TG and DSC curves of cupric carbonate ($CuCO_3{\cdot}Cu(OH)_2{\cdot}xH_2O$).

produced copper oxide with a weight loss proportion of 27.4%. Therefore, a temperature of 350 °C was chosen for the preparation of the Cu nanoparticles.

Regular TEM and HRTEM images are shown in Fig. 3. Obviously, the oblate spheroidal Cu nanoparticles were embedded in a matrix of carbon, and the size ranged from 50 to 80 nm. The space fringes detected in the HRTEM images (Fig. 3c) are well matched with the *d* value (0.208 nm) of Cu. The crystalline XRD pattern of the C/Cu sample (Fig. 3d) matches well with that of Cu nanoparticles (face-centered cubic, JCPDS 04-0836). No characteristic peaks for carbon were observed due to their amorphous nature.

The effect of the amount of glucose on the reduction product has been investigated. As Fig. 4 shows, in the presence of 0.10 g glucose, the XRD peaks were indexed to Cu_2O and Cu, and there also existed a weak unknown peak of an intermediate product from the reduction process. When the amount of glucose increased to 0.3 and 0.5 g, the Cu_2O peaks disappeared but the weak unknown peak remained. When the

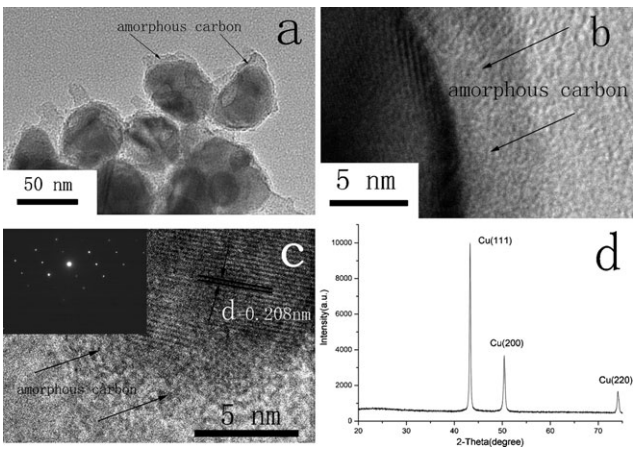

Fig. 3 (a) TEM image, (b,c) HRTEM images and (d) the XRD pattern of the C/Cu particles. The inset in (c) shows the electron diffraction scattering of the C/Cu particles. The carbon coating is indicated with arrows in all of the TEM and HRTEM images.

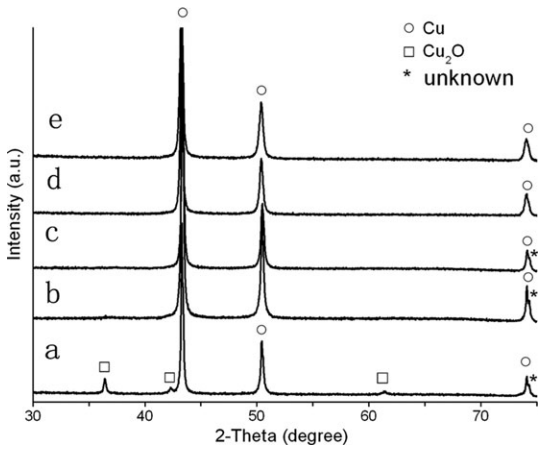

Fig. 4 XRD patterns of the C/Cu particles prepared by adding different amounts of glucose: (a) 0.10 g, (b) 0.30 g, (c) 0.50 g, (d) 1.00 g and (e) 1.50 g; the amount of cupric carbonate was 0.50 g.

amount of glucose was increased to 1.00 g, the weak unknown peak almost disappeared, and all of the peaks present belonged to face-centered cubic Cu nanoparticles. In addition, the dispersion ability (see the ESI†) of the product was improved with the increasing amount of glucose.

The Raman spectrum of the sample confirmed the presence of carbon on the Cu nanoparticles (Fig. 5). The peak at 1345 cm^{-1} (disordered D band) can be attributed to the A_{1g} model, and is associated with the presence of structural defects and disorder in the carbon material. The peak at 1580 cm^{-1} (G band) has E_{2g} symmetry and is related to the vibration of sp^2-bonded carbon atoms in a two-dimensional hexagonal lattice, resulting from the stretching modes of C═C bonds that are typical of graphite.[20,21]

The surface Plasmon band around 570 nm is characteristic of Cu nanoparticles (10 nm).[12,22] As Fig. 6 shows, the band for as-prepared oblate spheroidal C/Cu particles was red-shifted to 605 nm, which may be due to the interaction of the size and shape of the Cu nanoparticles with the carbon coating. The plasmon band was red-shifted to higher wavelengths with increasing particle size.[23,24] According to Schatz *et al.*,[25] the plasmon band depends strongly on particle shape, red-shifting as the particle becomes oblate.

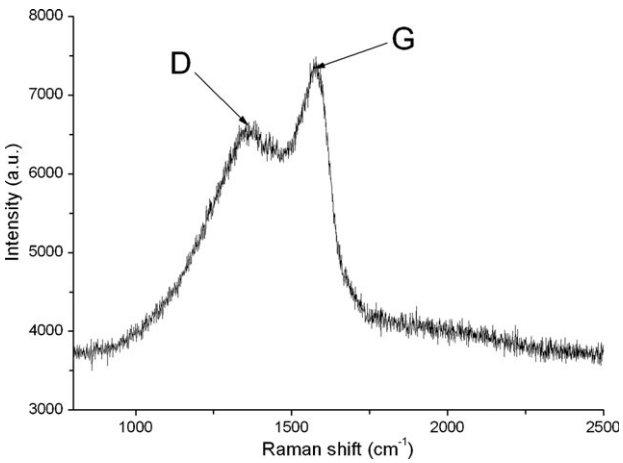

Fig. 5 The Raman spectrum of C/Cu particles.

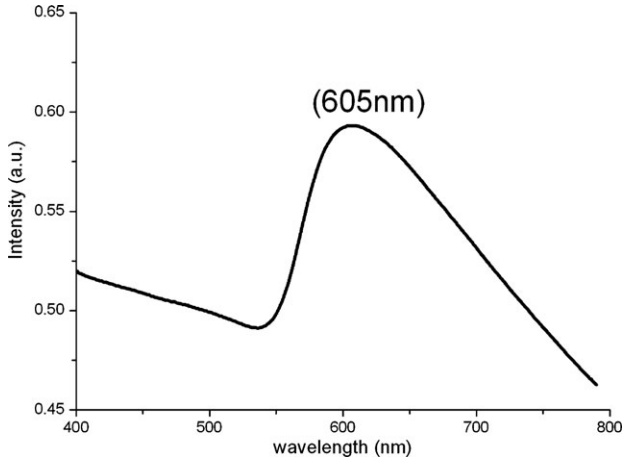

Fig. 6 Surface plasmon band of C/Cu particles.

In addition, the carbon coating also contributes to the red shift of the plasmon band, which is discussed as follows: For the C/Cu composite particles, the effective dielectric function of the surrounding medium around the C/Cu nanoparticles can be described by eqn (4):[26]

$$\varepsilon_{\text{eff}} = \varepsilon_{\text{water}}(1 - \Phi) + \varepsilon_{\text{carbon}}\Phi \quad (4)$$

where ε_{eff} is the effective dielectric constant of the medium surrounding the C/Cu nanoparticles, $\varepsilon_{\text{water}}$ is the dielectric constant of water, $\varepsilon_{\text{carbon}}$ is the dielectric constant of amorphous carbon and Φ is the volume fraction of the carbon layer. Because the refractive index of carbon (n_{carbon} = 1.6–2.0) is higher than that of water (n_{water} = 1.33), the carbon coating will induce the increase of ε_{eff} ($=n^2$). According to the Drude model,[10] the surface plasmon band position, λ, is related to the effective dielectric constant of the surrounding medium:

$$\lambda^2 = \lambda_p{}^2(\varepsilon^{\infty} + 2\varepsilon_{\text{eff}}) \quad (5)$$

where λ is the position of the plasmon band, ε^{∞} is the high frequency dielectric constant due to interband and core transitions, ε_{eff} is the effective dielectric constant of surrounding media, and λ_p is the metal's bulk plasma wavelength, which can be written as:

$$\lambda_p{}^2 = 4\pi^2c^2m\varepsilon_0/Ne^2 \quad (6)$$

where N is the concentration of free electrons in the metal, m is the effective mass of an electron and ε_0 is the vacuum dielectric constant. Therefore, the carbon coating induced the increase of ε_{eff} and resulted in the red shift of the plasmon band.

In conclusion, we have developed a simple solid-state reduction method to prepare C/Cu nanoparticles. Under the thermal treatment, the melting and carbonization of glucose formed carbon, which acted as a reducing agent and reduced copper ions to Cu nanoparticles, with carbon synchronously forming a layer around them. The synthesized C/Cu sample showed a plasmon resonance band that was red-shifted to 605 nm due to the influence of its size, shape and carbon coating.

The authors thank the Chinese Academy of Sciences and 973 Program for support.

Experimental

Materials

Glucose ($C_6H_{12}O_6{\cdot}H_2O$, AR) and cupric carbonate ($CuCO_3{\cdot}Cu(OH)_2{\cdot}xH_2O$, AR) were purchased from Beijing Chemical Factory (China) and used as received.

Synthesis

$CuCO_3{\cdot}Cu(OH)_2{\cdot}xH_2O$ (0.50 g) and $C_6H_{12}O_6{\cdot}H_2O$ (1.00 g) powders were mixed sufficiently through hand-griding in an agate mortar and heated at a 5 °C min^{-1} heating rate up to 350 °C in a tube furnace for 1 h, and then cooled to room temperature under nitrogen. C/Cu nanoparticles were thus obtained.

Characterization

Ultraviolet-visible (UV-vis) absorptions were recorded on a Shimadzu UV-1601 PC spectrophotometer. The C/Cu sample was sonicated in de-ionized water for 15 min and the obtained suspension was used for optical measurements.

TEM images were acquired on a JEM 2100F transmission electron microscope using an accelerating voltage of 200 kV. The sample was dispersed in ethanol by sonication and dropped onto a conventional carbon-coated Cu grid.

XRD patterns were obtained using a Bruker D8 Focus under Cu-K_α radiation of 1.54056 Å wavelength with a scanning speed of 4° min^{-1} in the 2θ range 20–75°.

Raman spectra were recorded on a Via-Reflex Raman system using a 632.8 nm excitation wavelength (He–Ne laser).

TG and DSC measurements were made under nitrogen on an STA 449 C instrument at a heating rate of 10 °C min^{-1}.

References

1 T. W. Ebbesen, H. J. Lezec, H. F. Ghaemi, T. Thio and P. A. Wolff, *Nature*, 1998, **391**, 667.
2 J. B. Pendry, *Phys. Rev. Lett.*, 2000, **85**, 3966.
3 S. A. Maier, M. L. Brongersma, P. G. Kik, S. Meltzer, A. A. G. Requicha and H. A. Atwater, *Adv. Mater.*, 2001, **13**, 1501.
4 S. A. Maier, P. G. Kik, H. A. Atwater, S. Meltzer, E. Harel, B. E. Koel and A. A. G. Requicha, *Nat. Mater.*, 2003, **2**, 229.
5 W. L. Barnes, A. Dereux and T. W. Ebbesen, *Nature*, 2003, **424**, 824.
6 S. Nie and S. R. Emory, *Science*, 1997, **275**, 1102.
7 K. Kneipp, Y. Wang, H. Kneipp, L. T. Perelman, I. Itzkan, R. R. Dasari and M. S. Feld, *Phys. Rev. Lett.*, 1997, **78**, 1667.
8 D. Dalacu and L. Martinu, *J. Appl. Phys.*, 2000, **87**, 228.
9 C. M. Liu, L. Guo, H. B. Xu, Z. Y. Wu and J. Weber, *Microelectron. Eng.*, 2003, **66**, 107.
10 P. Mulvaney, *Langmuir*, 1996, **12**, 788.
11 N. Kometani, M. Tsubonishi, T. Fujita, K. Asami and Y. Yonezawa, *Langmuir*, 2001, **17**, 578.
12 I. Lisiecki and M. P. Pileni, *J. Am. Chem. Soc.*, 1993, **115**, 3887.
13 I. Lisiecki and M. P. Pileni, *J. Phys. Chem.*, 1995, **99**, 5077.
14 I. Lisiecki, F. Billoudet and M. P. Pileni, *J. Mol. Liq.*, 1997, **72**, 251.
15 S. D. Bunge, T. J. Boyle and T. J. Headley, *Nano Lett.*, 2003, **3**, 901.
16 D. Ensign, M. Young and T. Douglas, *Inorg. Chem.*, 2004, **43**, 3441.
17 W. Krätschmer, L. D. Lamb, K. Fostiropoulos and D. R. Huffman, *Nature*, 1990, **347**, 354.
18 D. S. Jacob, I. Genish, L. Klein and A. Gedanken, *J. Phys. Chem. B*, 2006, **110**, 17711.

19 Y. Wang, L. Lin, B. S. Zhu, Y. X. Zhu and Y. C. Xie, *Appl. Surf. Sci.*, 2008, **254**, 6560.
20 Y. Li, E. J. Lee, W. P. Cai, K. Y. Kim and S. O. Cho, *ACS Nano*, 2008, **2**, 1108.
21 Y. Wang, F. B. Su, D. W. Colin, J. Y. Lee and X. S. Zhao, *Ind. Eng. Chem. Res.*, 2008, **47**, 2294.
22 A. Henglein, *J. Phys. Chem.*, 1993, **97**, 5457.
23 N. C. Bigall, T. Härtling, M. Klose, P. Simon, L. M. Eng and A. Eychmüller, *Nano Lett.*, 2008, **8**, 4588.
24 S. Link and M. A. El-Sayed, *J. Phys. Chem. B*, 1999, **103**, 4212.
25 K. L. Kelly, E. Coronado, L. L. Zhao and G. C. Schatz, *J. Phys. Chem. B*, 2003, **107**, 668.
26 Y. Wang, Y. Tan, S. H. Ding, L. Li and W. P. Qian, *Acta Chim. Sin.*, 2006, **64**, 2291.